Invert Neurosci (2008) 8:19–29
DOI 10.1007/s10158-007-0062-2

ORIGINAL PAPER

Study of nicotinic acetylcholine receptors on cultured antennal lobe neurones from adult honeybee brains

Guillaume Stéphane Barbara · Bernd Grünewald · Sandrine Paute · Monique Gauthier · Valérie Raymond-Delpech

Received: 27 July 2007 / Accepted: 25 October 2007 / Published online: 15 November 2007

Abstract In insects, acetylcholine (ACh) is the main neurotransmitter, and nicotinic acetylcholine receptors (nAChRs) mediate fast cholinergic synaptic transmission. In the honeybee, nAChRs are expressed in diverse structures including the primary olfactory centres of the brain, the antennal lobes (AL) and the mushroom bodies. Whole-cell, voltage-clamp recordings were used to characterize the nAChRs present on cultured AL cells from adult honeybee, *Apis mellifera*. In 90% of the cells, applications of ACh induced fast inward currents that desensitized slowly. The classical nicotinic agonists nicotine and imidacloprid elicited respectively 45 and 43% of the maximum ACh-induced currents. The ACh-elicited currents were blocked by nicotinic antagonists methyllycaconitine, dihydroxy-β-erythroidine and α-bungarotoxin. The nAChRs on adult AL cells are cation permeable channels. Our data indicate the existence of functional nAChRs on adult AL cells that differ from nAChRs on pupal Kenyon cells from mushroom bodies by their pharmacological profile and ionic permeability, suggesting that these receptors could be implicated in different functions.

Keywords Nicotinic acetylcholine receptor · Insect · Patch clamp · *Apis mellifera* · Antennal lobe

G. S. Barbara · S. Paute · M. Gauthier · V. Raymond-Delpech (✉)
Centre de Recherches sur la Cognition Animale-CNRS, Université Paul Sabatier, 118 rte de Narbonne, 31062 Toulouse, France
e-mail: raymond@cict.fr

B. Grünewald
Institut für Biologie AG Neurobiologie, Freie Universität Berlin, Königin-Luise Str. 28-30, 14195 Berlin, Germany

Introduction

Nicotinic acetylcholine receptors (nAChRs) mediate fast cholinergic synaptic transmission and are important excitatory neurotransmitter receptors in the central nervous system (CNS) of insects. Native neuronal nAChRs have been described in several insect species such as cockroaches (Harrow and Sattelle 1983; Van Eyseren et al. 1998; Courjaret et al. 2003; Salgado and Saar 2004), locusts (Albert and Lingle 1993; Hermsen et al. 1998; Jackson et al. 2002), crickets (Cayre et al. 1999), houseflies (Albert and Lingle 1993; Schmidt et al. 2000; Jepson et al. 2006), moths (Vermehren and Trimmer 2005) and honeybees (Goldberg et al. 1999; Déglise et al. 2002; Wustenberg and Grünewald 2004; Barbara et al. 2005). These insect nAChRs are targets for neonicotinoids, a major class of pesticides and especially imidacloprid (IMI), the main insecticide of this class (Matsuda et al. 2000; Tomizawa and Casida 2003).

Large parts of the insect olfactory pathway are cholinergic (Gorczyca and Hall 1984; Kreissl and Bicker 1989; Homberg et al. 1995; Homberg 2002; Yasuyama et al. 2002). In the honeybee, odours are detected by the olfactory receptor neurones (ORNs) in the antennae. ORNs axons arborize in the antennal lobe (AL) and synapse onto local interneurones (LINs) and projection neurones (PNs) (Hildebrand and Shepherd 1997). PNs transmit the olfactory information to higher-order brain centres, mainly to the lateral protocerebrum and the calyces of the mushroom bodies (Kirschner et al. 2006). In the calyces, the PNs make synaptic contacts with mushroom body intrinsic Kenyon cells. Acetylcholinesterase histochemistry, immunocytochemical staining for nAChRs, α-bungarotoxin (BGT) binding sites indicate cholinergic transmission in the AL and the existence of a cholinergic pathway via some

olfactory projections neurones into the mushroom bodies (Belzunces et al. 1988; Kreissl and Bicker 1989; Scheidler et al. 1990). As the LINs and PNs are targets of ORNs and Kenyon cells, they are possibly to express nAChRs (for review see Bicker 1999).

The development of primary cell cultures from pupal honeybee brains (Kreissl and Bicker 1992) has enabled easy access to individual cells to analyse their neurochemical phenotypes. Calcium imaging experiments performed on cultured pupal Kenyon cells revealed the presence of functional nAChRs (Bicker 1996). Moreover, in vitro patch-clamp studies on the somata of the same cells (Goldberg et al. 1999; Déglise et al. 2002; Grünewald et al. 2004; Wustenberg and Grünewald 2004) as well as those of pupal AL neurones (Barbara et al. 2005) showed that, in the honeybee as in many insects, nAChRs share several properties with vertebrate neuronal nAChRs, such as their pharmacology, cation selectivity and current inward rectification (Gundelfinger and Schulz 2000). They are sensitive to the nicotinic agonists nicotine (NIC), epibatidine and imidacloprid (IMI) (Déglise et al. 2002; Wustenberg and Grünewald 2004; Barbara et al. 2005) and to the nicotinic antagonists dihydroxy-β-erythroidine (DHE), methyllycaconitine (MLA) and α-bungarotoxin (BGT). In contrast to other insects (Thany et al. 2007), the presence of bungarotoxin-resistant nAChRs is not clearly demonstrated in honeybee but indirectly suggested (Gauthier et al. 2006). In the vertebrate nervous system DHE is a potent, but non-selective, nAChR antagonist (Dwoskin and Crooks 2001; Sharples and Wonnacott 2001) whereas MLA and BGT block mostly neuronal nAChRs composed of one of the α7–9 subunits (McGehee and Role 1995; Verbitsky et al. 2000; Millar 2003; Lecchi et al. 2004). To date, such pharmacological distinction has not been shown for insect neuronal receptors.

The bee brain contains several nAChR α subunits. Four different subunits (Amelα2, Amelα5, Amelα7 and Amelα8,) have been cloned and localized using in situ hybridization (Thany et al. 2003, 2005). The expression pattern in honeybee brain of each subunit was determined at different developmental stages. For example, the α7 subunit is not expressed by the non-compact Kenyon cells during pupal stage whereas it is expressed at adult stage (Thany et al. 2005). To date, the entire nAChR subunit gene family has been characterized from the honeybee genome and honeybee possesses nine α and two β nAChR subunits (Jones et al. 2006). These data suggest the existence of various native nAChRs in the honeybee brain, increasing the possibility that these receptors with different properties might be expressed at different developmental stages.

Behavioural pharmacological experiments showed that injections of the nicotinic antagonist mecamylamine into the honeybee brain disrupt the memory retrieval process (Lozano et al. 1996, 2001). Moreover, global injections of BGT and MLA specifically disrupt long-term memory formation (Dacher et al. 2005; Gauthier et al. 2006) whereas DHE injections only affect retrieval after short delays (Gauthier et al. 2006). Thus, cholinergic signalling appears to be involved in both memory formation and retrieval and suggest the existence of different nAChR subtypes which could be distinguished by their respective sensitivities to BGT, MLA and DHE. However, electrophysiological and calcium imaging studies of honeybee nAChRs from pupal brain tissue failed to distinguished distinct pharmacological profiles (Bicker and Kreissl 1994; Goldberg et al. 1999; Déglise et al. 2002; Wustenberg and Grünewald 2004; Barbara et al. 2005). These discrepancies between in vivo and in vitro data may be explained by the use of pupal cells for in vitro experiments, and adult animals for in vivo behavioural pharmacological experiments.

To get a better understanding of adult bee nAChRs and to enable a comparison with available in vivo pharmacological data, we have investigated the functional properties of nAChRs on adult cells dissociated from AL. Findings are compared with earlier works on pupal nAChRs of AL and mushroom body neurones with a view to bridging the gap between the behavioural roles and cellular physiology of these receptors.

Materials and methods

Animals and cell preparation

Honeybee colonies (*Apis mellifera*) were housed in a heated hut outside the laboratory. Adult honeybees were captured at the top of the hive and then anaesthetized by cooling at 4°C. Antennal lobes (AL) were dissected and AL cells were cultured following a modified version of a protocol originally developed by Kreissl and Bicker (1992). Brains were removed from the head capsule in a Leibovitz L15 medium (without L-glutamine, Cambrex Bio Science, Verviers, Belgium) supplemented with (in mM) 123 sucrose, 22.2 glucose, 13.9 fructose, 28.7 proline, 0.1 g l^{-1} streptomycin and 0.2 unit l^{-1} penicillin (pH 7.2; all chemicals from Sigma, St. Louis, MO, USA, unless otherwise stated). Head glands were removed and the AL were dissected out of the brains. All preparations were made under semi-sterile conditions, i.e. all preparation equipment was sterilised with 70% ethanol and solutions were filtered. The AL were incubated 45 min at 30°C in a dissociation saline (cell dissociation solution non-enzymatic 1×, Sigma) supplemented with protease (type IX from Bacillus polymyxa) and collagenase (type 1A from Clostridium histolyticum) 1 g l^{-1} each. They

were then transferred back in supplemented L15 medium and dissociated by very gentle trituration. Aliquots, equivalent to 2 AL, were then plated on poly-L-lysine coated glass coverslips (0.1 g l^{-1} poly-L-lysine, MW 150–300 kDa, pH 8.5—adjusted with NaOH) contained in culture dishes. Cells were allowed to settle and adhere to the substrate for at least 2 h at 26°C in an incubator at high humidity. The dishes were then filled with 2.5 ml of culture medium composed of 13% (v/v) heat inactivated foetal calf serum (Cambrex), 1.3% (v/v) yeast hydrolysate 50×, 19.1 mM glucose, 11.9 mM fructose, 24.7 mM proline, 125 mM sucrose, 2 mM L-glutamine and 50 µg ml^{-1} gentamicin, completed with L-15 medium (without L-glutamine, Cambrex) adjusted to pH 6.7 with NaOH. They were kept at 26°C in an incubator at high humidity. Cells were used for electrophysiological measurements after 2 days.

Electrophysiology

Whole-cell gigaohm seal recordings were performed at room temperature following the methods described by Hamill et al. (1981). Electrodes were pulled from borosilicate glass capillaries (1.5 mm o.d., 0.86 mm i.d., Harvard apparatus, Les Ulis, France) with a vertical puller (PP-850, Narishige Scientific Instrument Lab., Tokyo, Japan) and had tip resistances between 5 and 10 MΩ when filled with the pipette solution (see composition below). Recordings were made using an Axopatch 200B amplifier (Axon Instruments, Union City, CA, USA) connected to a DMA Labmaster (Scientific solutions Inc., Mentor, OH, USA) for data digitization. Pulse generation, data acquisition and analysis were carried out with JClamp 32 for Windows (version 12.5.0, J. Santos-Sacchi, SciSoft, USA). Currents were low-pass filtered at 1 kHz with a four-pole Bessel (−3 dB) filter and sampled at 1 kHz. Series resistances ranged between 5 and 50 MΩ and were compensated at approximately 80% when appropriate.

Perfusion and drug applications

A glass coverslip with attached cells was placed in a RC-25F perfusion chamber which has a bath volume of 500 µl (Harvard apparatus). The bath was continuously perfused at flow rates > 2 ml min^{-1} with a standard external solution that was composed of (in mM): 130 NaCl, 6 KCl, 4 $MgCl_2$, 5 $CaCl_2$, 185 sucrose, 25 glucose, 10 HEPES (pH 6.7 adjusted with NaOH). The internal solution contained (in mM): 120 KF, 18 KCl, 6 NaCl, 1 $CaCl_2$, 10 EGTA, 10 HEPES, 150 sucrose (pH 6.7 adjusted with KOH). There was no correction of the junction potential except for ion permeability determination.

Drugs were applied with a gravity fed fast perfusion system SF-77BST (Harvard Apparatus) that produces a constant fast solution exchange (<100 ms). This system contains a theta tube which had a tip size of 400 µm and was positioned at a distance of 100 µm from the studied cell. Agonists were applied during 2 s with an interval of 25 s between applications to avoid any cumulative receptor desensitization (Wustenberg and Grünewald 2004).

Concentration–response and inhibition curves

The agonists used were acetylcholine (ACh), ±nicotine (NIC) and imidacloprid (IMI). IMI was dissolved in DMSO with a final maximum concentration of 0.3% DMSO (v/v). For concentration–response curve determination, each agonist was applied in an increasing concentration order. For each concentration, the agonist was applied at least twice and the last two agonist-induced current peaks were averaged.

The antagonists used were α-bungarotoxin (BGT), methyllycaconitine (MLA) and dihydroxy-β-erythroidine (DHE), dissolved in standard external saline. At least two pulses of ACh were applied prior to the antagonist application. To obtain inhibition curves, each antagonist was applied in an increasing and successive concentration order. For each concentration, the antagonist was applied until maximum effect was reached (30 s to 3 min depending on the antagonist) and the last two agonist-induced current peaks were averaged. After the antagonist was tested, it was washed out and ACh was repeatedly applied until either the full current amplitude was reached or no further recovery of the current could be detected. Subsequently, only if the ACh-induced current fully recovers other antagonists could be tested, except in the case of BGT, since its block of the ACh-induced currents was only partly reversible. To compare current amplitudes, the peak amplitudes were normalized (I/I_{max}). Normalized data were fitted by use of GraphPad Prism (GraphPad Software, UK) to the following equation (Hill 1910; Weiss 1997):

$$\varphi = I_{min} + \frac{(I_{max} - I_{min})}{1+10^{(\log EC_{50} - [X])n_H}}$$

where X is the logarithm of the compound concentration, φ is the normalized response, I_{max} and I_{min} are the maximum and minimum normalized responses, respectively, EC_{50} is the concentration giving half the maximum normalized response and n_H is the Hill coefficient.

Reversal potential determination

The reversal potential of the ACh-induced currents was determined by measuring the peak current at various command potential steps between −100 mV and +60 mV (20 mV step increments). For these experiments, the external saline contained 100 nM tetrodotoxin (Tocris Cookson Ltd, Avnmouth, UK) to block voltage-activated sodium currents and 50 µM $CdCl_2$ to block voltage-activated calcium currents as already used by Goldberg et al. (1999). The internal saline contained 20 mM tetraethylammonium chloride to block some voltage-sensitive potassium currents (Schafer et al. 1994; Pelz et al. 1999). The reversal potential was calculated for each cell and averaged between cells.

The sodium permeability relative to the potassium (P_{Na}/P_K) and the calcium permeability relative to sodium (P_{Ca}/P_{Na}) were calculated using a form of the Goldman–Hodgkin–Katz (GHK) constant field relation (Jan and Jan 1976; Sands and Barish 1991):

$$E = \frac{RT}{F} \ln \frac{-b + \sqrt{b - 4ac}}{2a}$$

where

$$a = [K^+]_i + 4\frac{P_{Ca}}{P_K}[Ca^{2+}]_i + \frac{P_{Na}}{P_K}[Na^+]_i$$

$$b = [K^+]_i - [K^+]_o + \frac{P_{Na}}{P_K}([Na^+]_i - [Na^+]_o)$$

$$c = -[K^+]_o - \frac{P_{Na}}{P_K}[Na^+]_o - 4\frac{P_{Ca}}{P_K}[Ca^{2+}]_o$$

Ionic activities γ_i were employed and calculated using the Davies modification of the Extended Debye–Hückel equation (Davies 1962) in which the Debye factor A used is 0.509.

$$\log \gamma_i = -A \cdot z_i^2 \left(\frac{\sqrt{I}}{1 + \sqrt{I}} - 0.3I \right)$$

where

$$I = \frac{1}{2} \sum (c_i z_i^2)$$

with I ionic strength, c ionic concentration and z ionic valence.

Data analyses and statistics

Currents were low-pass filtered at 100 Hz (Gaussian type filter) after acquisition whenever appropriate. The time constants of current desensitization were measured using JClamp. The relative mean peak amplitude of each agonist-induced current was calculated by normalization to the current induced by 300 µM ACh. Standard error of the mean (SEM) is given throughout the text, unless otherwise stated. To test the reversibility of the antagonists, the ACh-induced currents before and after the antagonist application were compared using a Wilcoxon test. Drugs affinities and current reversal potentials were compared using a t test. Statistical analyses were performed with SPSS 12 (SPSS Inc., Chicago, IL, USA).

Results

Cell culture of adult antennal lobe neurones

Patch-clamp experiments were performed on AL neurones from adult honeybee brains (Fig. 1). Cultured cells survived for up to 1 month without culture medium renewal. Some cells had a cut-off axon. The somata diameter was approximately between 4 and 30 µm, which is similar to their size in the intact brain (Flanagan and Mercer 1989; Devaud and Masson 1999) and to that of pupal neurones, both in vitro and in vivo (Devaud et al. 1994; Sachse and Galizia 2002; Grünewald 2003). After 2 days of culture, no outgrowth could be observed (Fig. 1a), but after 11 days of culture short and thin dendrites grew (Fig. 1b).

Pharmacology of the nAChRs on adult honeybee antennal lobe neurones

Most of the recorded cells (170 out of 186) responded with a fast inward current to the application of 300 µM or 1 mM ACh at a holding potential of −110 mV. Among these cells two types of ACh-induced currents were observed. Type I currents were the most frequent and were found in 90% of the cells that responded whereas type II currents were found in 10% of the cells. Type I currents slowly desensitize (n = 152, Fig. 2a) compared to type II currents (n = 18, Fig. 2b). The decay phases of the ACh currents could be fitted with a single exponential function, yielding a time constant τ of 539 ± 81 ms (n = 45, with 300 µM ACh) for type I and τ of 32 ± 6 ms (n = 16, with 300 µM ACh) for type II. The peak amplitude of the maximum ACh-induced currents ranged between −9 pA and −355 pA with a mean peak amplitude of −69 ± 5 pA (n = 119) for type I currents and between −33 pA and −487 pA with a mean peak amplitude of −119 ± 26 pA (n = 17) for type II currents. Since type II currents were rarely measured, only the slow desensitizing current was further studied in detail and is described below.

Application of NIC and IMI onto AL cells elicited an inward current at a holding potential of −110 mV (Fig. 3a–d). Concentration–response curves for ACh, NIC

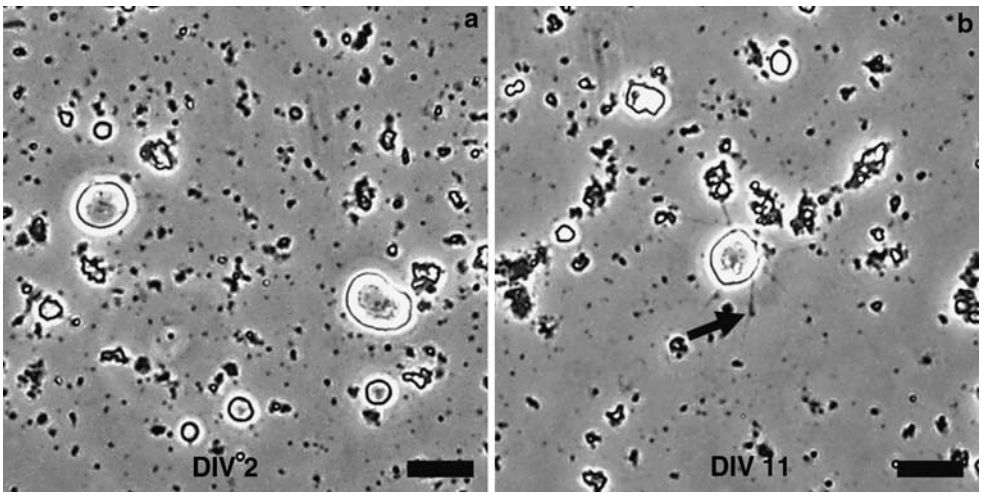

Fig. 1 Primary cell culture from adult honeybee antennal lobe after 2 (**a**) and 11 (**b**) days. Few neurones start to develop thin processes (*arrow*) after 7 days in vitro (DIV). These neurites continue growing throughout the period of 1 month. Phase contrast; *scale bars* 20 μm

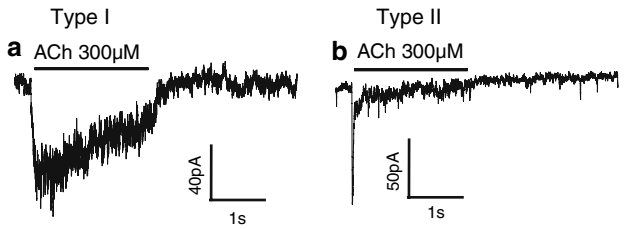

Fig. 2 Typical type I (**a**) and type II (**b**) ACh-induced currents (pulse duration 2 s, pulse potential −110 mV)

and IMI were determined and fitted. The maximal current amplitude was obtained at a concentration of 300 μM ACh; this concentration was then used as the standard for normalisation (I_{max}). The EC_{50} and Hill values were derived from the fitted curves (Fig. 3a–c, Table 1). Their EC_{50} give the following affinity ranking order: IMI (3.4 ± 0.26 μM) = NIC (3.76 ± 0.38 μM) > ACh (14.9 ± 1.2 μM) (IMI vs. NIC, $P = 0.93$, $t = 0.094$; IMI vs. ACh, $P = 0.0173$, $t = 2.674$; NIC vs. ACh, $P = 0.033$, $t = 2.365$). NIC and IMI are only partial agonists of nAChRs on AL neurones, since their efficacy to elicit inward currents is lower than that of ACh (Fig. 3d). At concentrations of 100 μM, for which NIC and IMI induced a maximum current, NIC induced 45 ± 18% ($n = 6$) and IMI 43 ± 19% ($n = 25$) of the maximum ACh-induced currents (300 μM, Fig. 3e). The mean peak currents and current densities of the maximum agonist-induced current are shown in Table 1.

The ACh-induced currents (300 μM ACh) could be blocked by application of MLA, DHE and BGT. At the highest concentration tested these antagonists completely blocked ACh-induced current. At lower concentrations, a concentration-dependent reduction of the ACh-induced current was observed (Fig. 4a–c). IC_{50} and Hill coefficients were estimated from inhibition curves (Fig. 4d, Table 1). MLA and DHE had closed but significantly different IC_{50} values with 1.4 ± 0.11 nM and 3.59 ± 0.43 nM ($P = 0.008$, $t = 3.232$), respectively, and their effects were fully reversible (Fig. 4b, c; for 100 nM MLA: $P = 0.61$, $Z = -0.507$, $n = 7$ and for 1 μM DHE: $P = 0.89$, $Z = -0.135$, $n = 5$). BGT was less efficient with an IC_{50} of 286 ± 13 nM (MLA vs. BGT, $P < 0.001$, $t = 15.61$; DHE vs. BGT, $P < 0.001$, $t = 8.273$) and its action was fully reversible at concentrations between 100 nM and 1 μM (not shown, at 1 μM, $P = 0.26$, $Z = -1.125$, $n = 6$), and was only partially reversible at 10 μM (Fig. 4a; $P = 0.028$, $Z = -2.201$, $n = 6$).

Relative ion permeabilities

The recordings obtained at different holding potentials (between −100 and +60 mV, +20 mV step increments) showed that depolarization reduced the maximum peak current amplitude. Current–voltage plot showed an inward rectification at potential more positive than +20 mV (Fig. 5). In standard saline (130 mM Na^+), the ionic current was inward for holding potential more negative than +10 mV. Using a linear regression method, the reversal potential of the ACh-induced current was estimated at +17.5 ± 2.6 mV ($n = 13$, Fig. 5a). Decreasing the sodium concentration of the external saline from 130 to 70 mM by replacing 60 mM NaCl by 60 mM TRIS chloride (TRIS-Cl) shifted the reversal potential to +1.1 ± 1.8 mV ($n = 6$) and reduced the current amplitude by 68.1 ± 4.1% ($n = 6$, $P = 0.028$, $Z = 2.201$). This result indicated that sodium was involved in the ACh-induced current. An estimate of the sodium to potassium permeability ratio (P_{Na}/P_K) under these ionic conditions was made by fitting its value in the

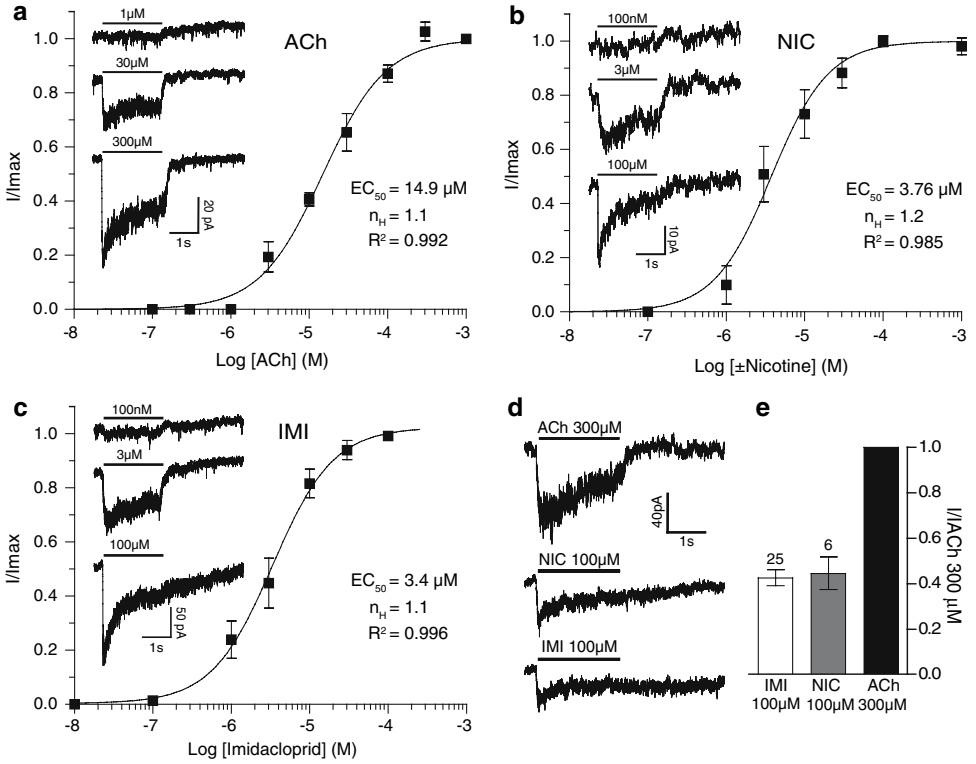

Fig. 3 Concentration–response curves of nicotinic agonists (**a**) ACh, (**b**) NIC and (**c**) IMI. Peak current amplitude induced by each agonist was measured and normalized to the maximum elicited current. Mean values ± standard deviation are plotted (n = 5–7 per point). The *smooth line* represents the best fit to the data. The EC_{50} and Hill coefficient values were estimated according to the Hill equation. *Insets* represent examples of the agonist-induced currents at the respective concentration (pulse duration: 2 s, holding potential −110 mV). Type I currents are elicited by the application of ACh, NIC or IMI (**d** pulse duration 2 s, pulse potential −110 mV). The quantification of the peak current amplitudes indicates that application of 100 μM NIC or IMI induced respectively 45 ± 4% (mean ± SEM, n = 6) and 43 ± 7% (mean ± SEM, n = 29) of the 300 μM ACh-induced current (**e**). Plotted are the normalized mean peak current amplitudes (relative to the current induced by 300 μM ACh)

Table 1 Characteristics of nAChRs. EC_{50}, IC_{50} and n_H values

	ACh	±Nicotine	Imidacloprid	BGT	MLA	DHE
EC_{50}	14.9 ± 1.2 μM	3.76 ± 0.38 μM	3.4 ± 0.26 μM			
IC_{50}				286 ± 13 nM	1.4 ± 0.11 nM	3.59 ± 0.43 nM
n_H	1.1	1.2	1.1	−1.8	−1.2	−0.7
Peak current (pA)	−69 ± 5 (n = 119)	−31 ± 7 (n = 6)	−35 ± 6 (n = 25)			
Current density (pA/pF)	−5.9 ± 0.4	−2.1 ± 0.9	−2.9 ± 0.4			

These values are the result of a fit of the data illustrated in Figs. 2 and 3, to the hill function. Mean peak currents and mean current density ± SEM are given for the agonists ACh (300 μM), NIC (100 μM) and IMI (100 μM) at the concentration inducing the maximum current

EC50 the concentration giving half the maximum normalized response, *IC50* the concentration giving half the maximum inhibition, n_H the estimated Hill coefficient, *ACh* acetylcholine, *BGT* α-bungarotoxin, *MLA* methyllycaconitine, *DHE* dihydroxy-β-erythroidine

GHK constant field relation to the observed reversal potentials. The best agreement with experimental data was obtained when P_{Na}/P_K = 1.61.

To determine whether nAChRs are permeable to calcium, we added 45 mM $CaCl_2$ to the standard external saline, increasing the calcium concentration from 5 mM (E_{Ca2+} = +40 mV) to 50 mM (E_{Ca2+} = +98 mV). But in that case, the chloride concentration also increases from 154 mM to 244 mM, the current–voltage plot of ACh responses obtained in saline solution containing 244 mM

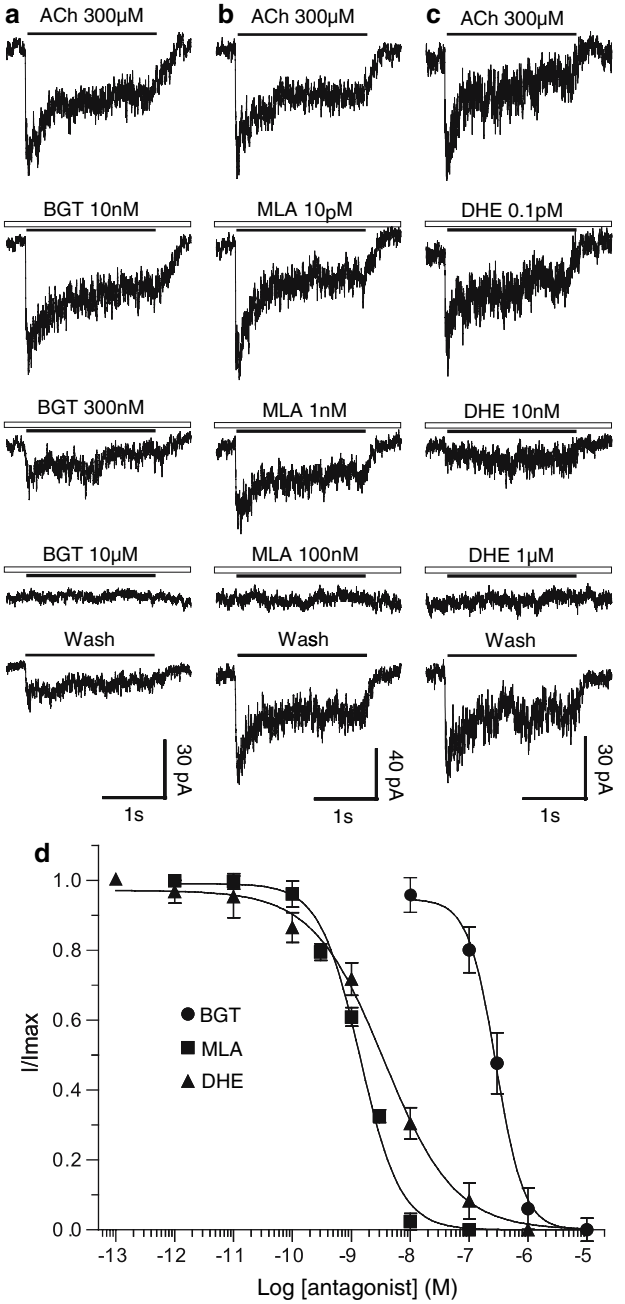

Fig. 4 Effects of nicotinic antagonists on ACh-induced currents. **a–c** Effect of increasing concentrations of (**a**) BGT, (**b**) MLA and (**c**) DHE on 300 µM ACh-induced currents (pulse duration: 2 s, holding potential −110 mV). Each column of currents was obtained from the same cell. The blockade by MLA and DHE was reversible. The full block by BGT was only partially reversible. **d** Inhibition curves of ACh-induced currents with the nicotinic antagonists BGT, MLA and DHE. Peak current amplitudes induced by application of 300 µM ACh during the antagonist application were measured and normalized to the current elicited before the antagonist application. Mean values ± standard deviation are plotted (n = 5–7 per point). According to the Hill equation, the *smooth line* represents the best fit to the data (R^2_{BGT} = 0.997, R^2_{MLA} = 0.995, R^2_{DHE} = 0.995). Values for IC_{50} and Hill coefficient are given in Table 1

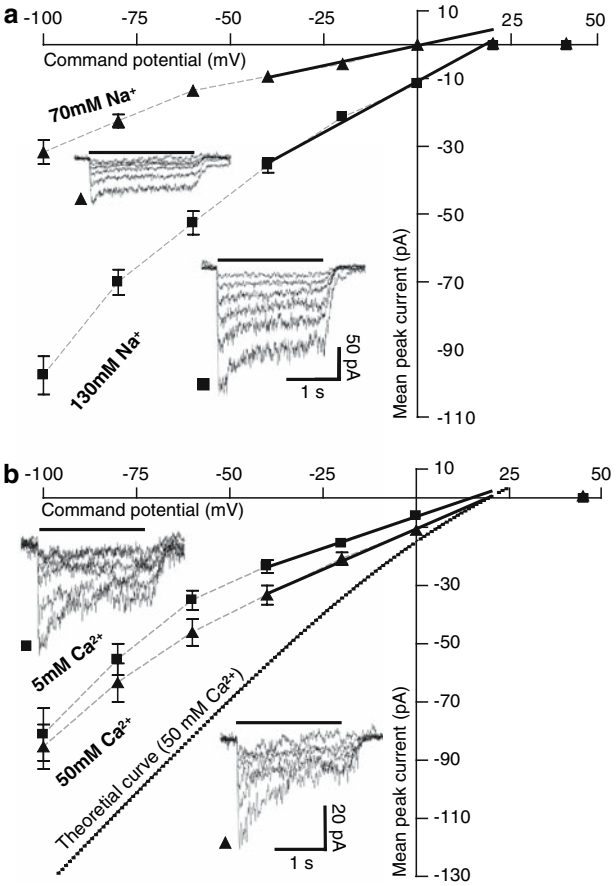

Fig. 5 Reversal potential determination of ACh-induced currents in saline solutions containing different sodium and calcium ion concentrations. **a** The ACh-elicited currents reversed at +17.5 ± 2.6 mV (n = 13) for 130 mM Na^+ (*standard saline*). For 70 mM Na^+, the ACh-induced current reversal potential shifted to +1.1 ± 1.8 mV (n = 6). NaCl was substituted by TRIS-Cl. **b** The ACh-induced currents reversed at +16.9 ± 3.8 mV (n = 7) for 5 mM Ca^{2+}. At 50 mM Ca^{2+}, the ACh-induced currents reversal potential shifted to +17.9 ± 1.9 mV (n = 11). Chloride concentration was 244 mM for both experiments and adjusted with TRIS-Cl. Osmolarity was adjusted with sucrose. *Black doted line* represents the theoretical curve calculated by the use of GHK current equation and of estimated ion ratio permeability; ACh-induced current intensity in standard saline was used as reference. *Insets* represent examples of the ACh-induced currents at membrane potential from −100 to 0 mV by increments of 20 mV (pulse duration: 2 s). Mean values ± SEM are plotted, (**b**) mean peak current at +20 mV potential is null and is not represented for figure clarity. The *black line* represents the linear regression for points −40, −20 and 0 mV

chloride and 5 mM calcium was compared to that obtained in a solution containing 244 mM chloride and 50 mM calcium.

In external saline solution (244 mM Cl^-, 5 mM Ca^{2+}), the reversal potential was estimated at +15.2 ± 3.4 mV (n = 7). When the external calcium concentration was increased, the reversal potential shifted by +2.7 mV to

+17.9 ± 1.9 mV (Fig. 5b, $n = 11$). An estimate of the calcium to potassium permeability ratio (P_{Ca}/P_K) under these ionic conditions was made, the best agreement with experimental data was obtained when $P_{Ca}/P_K = 0.87$. Ignoring the effects of surface charge (Green and Andersen 1991), calcium to sodium permeability ratio (P_{Ca}/P_{Na}) was estimated as 0.54.

Discussion

Pharmacology of adult honeybee antennal lobe nAChRs

Our study shows that adult AL neurones express functional nAChRs. These data support immunohistochemical reports (Bicker 1999) indicating cholinergic neurotransmission within the mature honeybee AL. In our study, most of the recorded honeybee AL cells in culture responded to applications of ACh and other nicotinic agonists with a fast inward current (type I). The nicotinic agonists NIC and IMI are partial agonists. Their affinities were estimated and gave the following rank order IMI = NIC > ACh. The ACh-elicited currents were blocked by nAChR antagonists with the efficacy rank order: MLA ≥ DHE > BGT. In addition we determined that the ACh-induced currents were cationic. This profile strongly suggests that these ACh receptors are nicotinic (for review on insect nAChRs see Gundelfinger 1992; Osborne 1996; Gundelfinger and Schulz 2000; Tomizawa and Casida 2001; Thany et al. 2007).

This pharmacology is similar to other insect nAChRs. The EC_{50} value for ACh recorded on bee AL neurones (14.9 μM) is in the same range as other insect nAChRs for which EC_{50}s range between 10 μM and 30 μM (David and Sattelle 1984; Albert and Lingle 1993; van den Beukel et al. 1998; Van Eyseren et al. 1998; Brown et al. 2006). In our study, as for other insect nAChRs, NIC and IMI are partial agonists (Orr et al. 1997; Hermsen et al. 1998; Brown et al. 2006; Jepson et al. 2006). However, on cockroach DUM neurones NIC may be a full agonist (Lapied et al. 1990). The effective antagonists on honeybee nAChRs are also effective in other insect preparations (David and Sattelle 1984; Lapied et al. 1990; Orr et al. 1997; Van Eyseren et al. 1998; Cayre et al. 1999; Schmidt et al. 2000; Salgado and Saar 2004; Gu and O'Dowd 2006; Jepson et al. 2006). Nevertheless BGT-insensitive nAChRs were described in cockroaches (Bai et al. 1992; David and Pitman 1993; Courjaret et al. 2003), grasshoppers (Goodman and Spitzer 1980) and moths (Fickbohm and Trimmer 2003).

On AL neurones, the pharmacology of ACh-induced currents of adult cells is slightly different to that of the pupal currents (Barbara et al. 2005). On adult cells the antagonist action of 1 μM BGT was fully reversible whereas on pupal cells it was only partially reversible. NIC and IMI induced slightly smaller and less variable currents on pupal AL cells. This greater variability of the IMI-induced currents (from 15 to 60% of the ACh-induced currents) on adult cells suggests the existence of different nAChR types for which IMI appears as a partial agonist but with different potencies. The existence of two different IMI-elicited currents was reported on AL cells from adult honeybee (Nauen et al. 2001). In that case, IMI acted either as a full agonist for one cell population or as a partial agonist for another one. In our case, such a clear distinction was not observed. This discrepancy between this previous study and ours may be due to the use of different experimental conditions and/or different cells. Our recordings were made after 2 days in culture whereas Nauen et al. has recorded at 2 days. The honeybee AL is composed of local neurones and projections neurones. It may well be that Nauen et al. (2001) and we recorded from different cell types. Consistent with this hypothesis Nauen et al. (2001) reported cell sizes ranging between 30 and 50 μm which are larger than our observation (4–30 μm). In addition, ACh-induced currents were larger in their study (ACh 100 μM; between −30 and −1,600 pA) than in ours (ACh 300 μM or 1 mM; −9 to −355 pA). All these data suggest that different nAChRs could exist on distinct AL cells but also on one type of cells.

Nicotinic AChRs were also studied on honeybee pupal Kenyon cells in culture (Bicker and Kreissl 1994; Goldberg et al. 1999; Déglise et al. 2002; Wustenberg and Grünewald 2004). On these cells NIC and IMI were partial agonists with a lower efficacy in comparison to the present study. ACh and NIC had a higher affinity and IMI a lower affinity on pupal cells suggesting different nAChR types on AL cells and pupal Kenyon cells. Two studies on pupal Kenyon cells showed a full or nearly full blockade of ACh-elicited currents by the application of 1 μM BGT (Goldberg et al. 1999; Déglise et al. 2002), which is close to the blockade of 89% observed in the present study. However, a striking difference is the different potency of MLA and DHE, which are respectively 58- and 7,200-fold more effective on pupal Kenyon cells than on adult AL neurones (Wustenberg and Grünewald 2004). Consequently, DHE may be a useful tool to distinguish different nAChR subtypes expressed in AL and Kenyon cells. This pharmacological difference between adult AL cells and pupal Kenyon cells could be due to differences in nAChRs subunits expression (Thany et al. 2003, 2005) and/or to editing and alternative splicing in the nAChRs genes (Jones et al. 2006). In agreement with the divergent ACh-induced current pharmacological profiles, in situ hybridization experiments revealed differences in subunit expression

between mushroom bodies and AL in adults (Thany et al. 2005). Taken together, these data suggest the existence of various nAChR types in the honeybee brain.

Cation permeability ratios

Using voltage steps, the reversal potential of ACh-induced currents was estimated to +17.5 mV, a value indicating that the nAChR is a non-selective cationic channel. This finding is in agreement with previous observations on a large number of insect preparations (Benson 1992; Cayre et al. 1999; Jackson et al. 2002). The sodium to potassium permeability ratio (P_{Na}/P_K) was estimated to 1.61 by varying extracellular ionic sodium concentrations; to our knowledge, such a high P_{Na}/P_K was not reported before and the physiological role of such high P_{Na}/P_K value remains to be elucidated.

The calcium to sodium permeability ratio of the studied nAChR is smaller than that estimated for the pupal Kenyon cell nAChRs (Goldberg et al. 1999) but similar to that estimated for *Periplaneta americana* embryonic neurones (Van Eyseren et al. 1998). According to the extended GHK current equations (Sands and Barish 1992), increasing external calcium concentration would increase the ionic current at negative potentials (see theoretical curve; Fig. 5b). In contrast, in the present study a decrease was observed, as reported in others' preparations (Adams and Nutter 1992; Sands and Barish 1992). For vertebrates neuronal nAChRs, it was shown that calcium can regulate the homomeric α7 nAChR via calcium-binding sites (Galzi et al. 1996). Such a mechanism might explain our observed ACh-induced current decrease. In vertebrates, P_{Ca}/P_{Na} allowed neuronal heteromeric and homomeric nAChRs to be distinguished: homomeric receptors solely composed of α subunit have a high P_{Ca}/P_{Na} whereas heteromeric nAChRs ($\alpha_4\beta_2$) have a lower P_{Ca}/P_{Na} (Fucile 2004). In the pupal honeybee, nAChRs on Kenyon cells have high P_{Ca}/P_{Na}, therefore resemble more the neuronal homomeric vertebrate nAChRs, whereas nAChRs on antennal cells of adult honeybee have a lower P_{Ca}/P_{Na}, therefore they resemble more the vertebrate neuronal heteromeric nAChRs.

Functional implications and conclusions

Using pharmacological tools, behavioural studies showed the implication of diverse nAChRs in learning and memory processes (Dacher et al. 2005; Gauthier et al. 2006). In particular, the behavioural effects of MLA and BGT could be dissociated from those of DHE following injection of the drugs into the entire brain. We may hypothesize that different neuronal populations of the adult honeybee brain possess nAChRs with different sensitivities to these blockers. To understand these learning and memory processes, the identification of both the nAChR types involved and the cell types bearing these nAChRs is important. The next step will be to isolate the nAChRs subunits involved in the ACh-induced current measured taking advantage of the full sequencing of the bee genome (The Honeybee Genome Sequencing Consortium 2006). All subunits were sequenced, and they are currently being cloned (Thany et al. 2003, 2005; Jones et al. 2006). Molecular tools should help to determine the involvement of each nAChR subunit in the ACh-induced currents observed. Since the expression of insect subunits in heterologous system is difficult to realize (Tomizawa and Casida 2001), clear links between the pharmacology of native nAChRs and their subunit composition still need to be elucidated. To by-pass this difficulty, the use of single cell RT-PCR on native cells (Klink et al. 2001) combined with RNA interference against specific subunits (Vermehren et al. 2001; Fickbohm and Trimmer 2003; Vermehren and Trimmer 2005) might be explored.

Acknowledgments The authors thank M. Moreau for help on ion permeability determination; M. Lambin, C. Armengaud, J. M. Devaud and J. C. Sandoz for suggestions on figures and manuscript; and M. Bazelot for kindly sharing cell cultures. G. S. Barbara was supported by a doctoral grant from the French Ministry of Scientific Research and Education. This work benefited from financial support of the European Community in the frame of the Apiculture Program 2007, Agreement 07–09 between Vinifhlor, CNRS and UPS.

References

Adams DJ, Nutter TJ (1992) Calcium permeability and modulation of nicotinic acetylcholine receptor-channels in rat parasympathetic neurons. J Physiol Paris 86:67–76

Albert JL, Lingle CJ (1993) Activation of nicotinic acetylcholine receptors on cultured *Drosophila* and other insect neurones. J Physiol 463:605–630

Bai D, Erdbrugger H, Breer H, Sattelle DB (1992) Acetylcholine receptors of thoracic dorsal midline neurones in the cockroach, *Periplaneta americana*. Arch Insect Biochem Physiol 21:289–301

Barbara GS, Zube C, Rybak J, Gauthier M, Grünewald B (2005) Acetylcholine, GABA and glutamate induce ionic currents in cultured antennal lobe neurons of the honeybee, *Apis mellifera*. J Comp Physiol A Neuroethol Sens Neural Behav Physiol 191:823–836

Belzunces LP, Toutant JP, Bounias M (1988) Acetylcholinesterase from *Apis mellifera* head. Evidence for amphiphilic and hydrophilic forms characterized by Triton X-114 phase separation. Biochem J 255:463–470

Benson JA (1992) Electrophysiological pharmacology of the nicotinic and muscarinic cholinergic responses of isolated neuronal somata from locust thoracic ganglia. J Exp Biol 170:203–233

Bicker G (1996) Transmitter-induced calcium signalling in cultured neurons of the insect brain. J Neurosci Methods 69:33–41

Bicker G (1999) Histochemistry of classical neurotransmitters in antennal lobes and mushroom bodies of the honeybee. Microsc Res Tech 45:174–183

Bicker G, Kreissl S (1994) Calcium imaging reveals nicotinic acetylcholine receptors on cultured mushroom body neurons. J Neurophysiol 71:808–810

Brown LA, Ihara M, Buckingham SD, Matsuda K, Sattelle DB (2006) Neonicotinoid insecticides display partial and super agonist actions on native insect nicotinic acetylcholine receptors. J Neurochem 99:608–615

Cayre M, Buckingham SD, Yagodin S, Sattelle DB (1999) Cultured insect mushroom body neurons express functional receptors for acetylcholine, GABA, glutamate, octopamine, and dopamine. J Neurophysiol 81:1–14

Courjaret R, Grolleau F, Lapied B (2003) Two distinct calcium-sensitive and -insensitive PKC up- and down-regulate an α-bungarotoxin-resistant nAChR1 in insect neurosecretory cells (DUM neurons). Eur J Neurosci 17:2023–2034

Dacher M, Lagarrigue A, Gauthier M (2005) Antennal tactile learning in the honeybee: effect of nicotinic antagonists on memory dynamics. Neuroscience 130:37–50

David JA, Sattelle DB (1984) Actions of cholinergic pharmacological agents on the cell body membrane of the fast coxal depressor motoneurone of the cockroach (*Periplaneta americana*). J Exp Biol 108:119–136

David JA, Pitman RM (1993) The pharmacology of a-bungarotoxin-resistant acetylcholine receptors on an identified cockroach motoneurone. J Comp Physiol A Neuroethol Sens Neural Behav Physiol 172:359–368

Davies CW (1962) Ion association. Butterworths, London

Déglise P, Grünewald B, Gauthier M (2002) The insecticide imidacloprid is a partial agonist of the nicotinic receptor of honeybee Kenyon cells. Neurosci Lett 321:13–16

Devaud JM, Masson C (1999) Dendritic pattern development of the honeybee antennal lobe neurons: a laser scanning confocal microscopic study. J Neurobiol 39:461–474

Devaud JM, Quenet B, Gascuel J, Masson C (1994) A morphometric classification of pupal honeybee antennal lobe neurones in culture. Neuroreport 6:214–218

Dwoskin LP, Crooks PA (2001) Competitive neuronal nicotinic receptor antagonists: a new direction for drug discovery. J Pharmacol Exp Ther 298:395–402

Fickbohm D, Trimmer BA (2003) Antisense inhibition of neuronal nicotinic receptors in the tobacco-feeding insect, *Manduca sexta*. Arch Insect Biochem Physiol 53:172–185

Flanagan D, Mercer AR (1989) Morphology and response characteristics of neurones in the deutocerebrum of the brain in the honeybee *Apis mellifera*. J Comp Physiol A 164:483–494

Fucile S (2004) Ca^{2+} permeability of nicotinic acetylcholine receptors. Cell Calcium 35:1–8

Galzi JL, Bertrand S, Corringer PJ, Changeux JP, Bertrand D (1996) Identification of calcium binding sites that regulate potentiation of a neuronal nicotinic acetylcholine receptor. Embo J 15:5824–5832

Gauthier M, Dacher M, Thany SH, Niggebrugge C, Déglise P, Kljucevic P, Armengaud C, Grünewald B (2006) Involvement of α-bungarotoxin-sensitive nicotinic receptors in long-term memory formation in the honeybee (*Apis mellifera*). Neurobiol Learn Mem

Goldberg F, Grünewald B, Rosenboom H, Menzel R (1999) Nicotinic acetylcholine currents of cultured Kenyon cells from the mushroom bodies of the honey bee *Apis mellifera*. J Physiol 514(Pt 3):759–768

Goodman CS, Spitzer NC (1980) Embryonic development of neurotransmitter receptors in grasshoppers. In: Sattelle DB, Hall LM, Hildebrand JG (eds) Receptors for neurotransmitters, hormones and pheromones in insects. Elsevier/North-Holland Biochemical, Amsterdam, pp 195–207

Gorczyca M, Hall JC (1984) Identification of a cholinergic synapse in the giant fiber pathway of *Drosophila* using conditional mutations of acetylcholine synthesis. J Neurogenet 1:289–313

Green WN, Andersen OS (1991) Surface charges and ion channel function. Annu Rev Physiol 53:341–359

Grünewald B (2003) Differential expression of voltage-sensitive K^+ and Ca^{2+} currents in neurons of the honeybee olfactory pathway. J Exp Biol 206:117–129

Grünewald B, Wersing A, Wustenberg DG (2004) Learning channels: cellular physiology of odor processing neurons within the honeybee brain. Acta Biol Hung 55:53–63

Gu H, O'Dowd DK (2006) Cholinergic synaptic transmission in adult *Drosophila* Kenyon cells in situ. J Neurosci 26:265–272

Gundelfinger ED (1992) How complex is the nicotinic receptor system of insects? Trends Neurosci 15:206–211

Gundelfinger ED, Schulz R (2000) Insect nicotinic acetylcholine receptors: genes, structure, physiological and pharmacological properties. In: Clementi F, Fornasari D, Gotti C (eds) Handbook of experimental pharmacology, neuronal nicotinic receptors. Springer, Berlin, pp 496–521

Hamill OP, Marty A, Neher E, Sakmann B, Sigworth FJ (1981) Improved patch-clamp techniques for high-resolution current recording from cells and cell-free membrane patches. Pflugers Arch 391:85–100

Harrow ID, Sattelle DB (1983) Acetylcholine receptors on the cell body membrane of giant interneurone 2 in the cockroach, *Periplaneta americana*. J Exp Biol 105:339–350

Hermsen B, Stetzer E, Thees R, Heiermann R, Schrattenholz A, Ebbinghaus U, Kretschmer A, Methfessel C, Reinhardt S, Maelicke A (1998) Neuronal nicotinic receptors in the locust *Locusta migratoria*: cloning and expression. J Biol Chem 273:18394–18404

Hildebrand JG, Shepherd GM (1997) Mechanisms of olfactory discrimination: converging evidence for common principles across phyla. Annu Rev Neurosci 20:595–631

Hill AV (1910) The possible effects of the aggregation of the molecules of haemoglobin on its dissociation curves. J Physiol 40:4–7

Homberg U (2002) Neurotransmitters and neuropeptides in the brain of the locust. Microsc Res Tech 56:189–209

Homberg U, Hoskins SG, Hildebrand JG (1995) Distribution of acetylcholinesterase activity in the deutocerebrum of the sphinx moth *Manduca sexta*. Cell Tissue Res 279:249–259

Jackson C, Bermudez I, Beadle DJ (2002) Pharmacological properties of nicotinic acetylcholine receptors in isolated *Locusta migratoria* neurones. Microsc Res Tech 56:249–255

Jan LY, Jan YN (1976) L-glutamate as an excitatory transmitter at the *Drosophila* larval neuromuscular junction. J Physiol 262:215–236

Jepson JE, Brown LA, Sattelle DB (2006) The actions of the neonicotinoid imidacloprid on cholinergic neurons of *Drosophila melanogaster*. Invert Neurosci 6:33–40

Jones AK, Raymond-Delpech V, Thany SH, Gauthier M, Sattelle DB (2006) The nicotinic acetylcholine receptor gene family of the honey bee, *Apis mellifera*. Genome Res 16:1422–1430

Kirschner S, Kleineidam CJ, Zube C, Rybak J, Grünewald B, Rossler W (2006) Dual olfactory pathway in the honeybee, *Apis mellifera*. J Comp Neurol 499:933–952

Klink R, de Kerchove d'Exaerde A, Zoli M, Changeux JP (2001) Molecular and physiological diversity of nicotinic acetylcholine receptors in the midbrain dopaminergic nuclei. J Neurosci 21:1452–1463

Kreissl S, Bicker G (1989) Histochemistry of acetylcholinesterase and immunocytochemistry of an acetylcholine receptor-like antigen in the brain of the honeybee. J Comp Neurol 286:71–84

Kreissl S, Bicker G (1992) Dissociated neurons of the pupal honeybee brain in cell culture. J Neurocytol 21:545–556

Lapied B, Le Corronc H, Hue B (1990) Sensitive nicotinic and mixed nicotinic-muscarinic receptors in insect neurosecretory cells. Brain Res 533:132–136

Lecchi M, Marguerat A, Ionescu A, Pelizzone M, Renaud P, Sommerhalder J, Safran AB, Tribollet E, Bertrand D (2004) Ganglion cells from chick retina display multiple functional nAChR subtypes. Neuroreport 15:307–311

Lozano VC, Bonnard E, Gauthier M, Richard D (1996) Mecamylamine-induced impairment of acquisition and retrieval of olfactory conditioning in the honeybee. Behav Brain Res 81:215–222

Lozano VC, Armengaud C, Gauthier M (2001) Memory impairment induced by cholinergic antagonists injected into the mushroom bodies of the honeybee. J Comp Physiol [A] 187:249–254

Matsuda K, Shimomura M, Kondo Y, Ihara M, Hashigami K, Yoshida N, Raymond V, Mongan NP, Freeman JC, Komai K, Sattelle DB (2000) Role of loop D of the α7 nicotinic acetylcholine receptor in its interaction with the insecticide imidacloprid and related neonicotinoids. Br J Pharmacol 130:981–986

McGehee DS, Role LW (1995) Physiological diversity of nicotinic acetylcholine receptors expressed by vertebrate neurons. Annu Rev Physiol 57:521–546

Millar NS (2003) Assembly and subunit diversity of nicotinic acetylcholine receptors. Biochem Soc Trans 31:869–874

Nauen R, Ebbinghaus-Kintscher U, Schmuck R (2001) Toxicity and nicotinic acetylcholine receptor interaction of imidacloprid and its metabolites in *Apis mellifera* (Hymenoptera: Apidae). Pest Manag Sci 57:577–586

Orr N, Shaffner AJ, Watson GB (1997) Pharmacological characterization of an epibatidine binding site in the nerve cord of *Periplaneta americana*. Pesticide Biochem Physiol 58:183–192

Osborne RH (1996) Insect neurotransmission: neurotransmitters and their receptors. Pharmacol Ther 69:117–142

Pelz C, Jander J, Rosenboom H, Hammer M, Menzel R (1999) IA in Kenyon cells of the mushroom body of honeybees resembles shaker currents: kinetics, modulation by K^+, and simulation. J Neurophysiol 81:1749–1759

Sachse S, Galizia CG (2002) Role of inhibition for temporal and spatial odor representation in olfactory output neurons: a calcium imaging study. J Neurophysiol 87:1106–1117

Salgado VL, Saar R (2004) Desensitizing and non-desensitizing subtypes of α-bungarotoxin-sensitive nicotinic acetylcholine receptors in cockroach neurons. J Insect Physiol 50:867–879

Sands SB, Barish ME (1991) Calcium permeability of neuronal nicotinic acetylcholine receptor channels in PC12 cells. Brain Res 560:38–42

Sands SB, Barish ME (1992) Neuronal nicotinic acetylcholine receptor currents in phaeochromocytoma (PC12) cells: dual mechanisms of rectification. J Physiol 447:467–487

Schafer S, Rosenboom H, Menzel R (1994) Ionic currents of Kenyon cells from the mushroom body of the honeybee. J Neurosci 14:4600–4612

Scheidler A, Kaulen P, Bruning G, Erber J (1990) Quantitative autoradiographic localization of [125I] α-bungarotoxin binding sites in the honeybee brain. Brain Res 534:332–335

Schmidt H, Luer K, Hevers W, Technau GM (2000) Ionic currents of *Drosophila* embryonic neurons derived from selectively cultured CNS midline precursors. J Neurobiol 44:392–413

Sharples CGV, Wonnacott S (2001) Neuronal nicotinic receptors. Tocris reviews, vol 19

Thany SH, Lenaers G, Crozatier M, Armengaud C, Gauthier M (2003) Identification and localization of the nicotinic acetylcholine receptor α3 mRNA in the brain of the honeybee, *Apis mellifera*. Insect Mol Biol 12:255–262

Thany SH, Crozatier M, Raymond-Delpech V, Gauthier M, Lenaers G (2005) Apisα2, Apisα7–1 and Apisα7–2: three new neuronal nicotinic acetylcholine receptor α-subunits in the honeybee brain. Gene 344:125–132

Thany SH, Lenaers G, Raymond-Delpech V, Sattelle DB, Lapied B (2007) Exploring the pharmacological properties of insect nicotinic acetylcholine receptors. Trends Pharmacol Sci 28:14–22

The Honeybee Genome Sequencing Consortium (2006) Insights into social insects from the genome of the honeybee *Apis mellifera*. Nature 442:931

Tomizawa M, Casida JE (2001) Structure and diversity of insect nicotinic acetylcholine receptors. Pest Manag Sci 57:914–922

Tomizawa M, Casida JE (2003) Selective toxicity of neonicotinoids attributable to specificity of insect and mammalian nicotinic receptors. Annu Rev Entomol 48:339–364

van den Beukel I, van Kleef RG, Oortgiesen M (1998) Differential effects of physostigmine and organophosphates on nicotinic receptors in neuronal cells of different species. Neurotoxicology 19:777–787

Van Eyseren I, Guillet JC, Le Guen J, Tiaho F, Pichon Y (1998) Effects of nicotinic and muscarinic ligands on embryonic neurones of *Periplaneta americana* in primary culture: a whole cell clamp study. J Insect Physiol 44:227–240

Verbitsky M, Rothlin CV, Katz E, Elgoyhen AB (2000) Mixed nicotinic-muscarinic properties of the α9 nicotinic cholinergic receptor. Neuropharmacology 39:2515–2524

Vermehren A, Qazi S, Trimmer BA (2001) The nicotinic α subunit MARA1 is necessary for cholinergic evoked calcium transients in *Manduca* neurons. Neurosci Lett 313:113–116

Vermehren A, Trimmer BA (2005) Expression and function of two nicotinic subunits in insect neurons. J Neurobiol 62:289–298

Weiss JN (1997) The Hill equation revisited: uses and misuses. Faseb J 11:835–841

Wustenberg DG, Grünewald B (2004) Pharmacology of the neuronal nicotinic acetylcholine receptor of cultured Kenyon cells of the honeybee, *Apis mellifera*. J Comp Physiol A Neuroethol Sens Neural Behav Physiol 190:807–821

Yasuyama K, Meinertzhagen IA, Schurmann FW (2002) Synaptic organization of the mushroom body calyx in *Drosophila melanogaster*. J Comp Neurol 445:211–226